IMPACT RESISTANT DESIGNS FROM THE CUTICLE OF THE MANTIS SHRIMP

Nicholas A. Yaraghi[1], Nicolás Guarín-Zapata[2], David Restrepo Arango[2], Steven Herrera[1], Jesus Rivera[1], Pablo Zavattieri[2] and David Kisailus[1,3]

[1]Materials Science and Engineering, University of California, Riverside, Riverside, CA, United States
Emails: nyara001@ucr.edu, sherr006@ucr.edu, jrive021@ucr.edu, webpage: http://www.mse.ucr.edu/

[2]Civil Engineering, Purdue University, West Lafayette, IN, United States
Emails: nguarin@purdue.edu, drestrep@purdue.edu, zavattie@purdue.edu, webpage: https://engineering.purdue.edu/CE

[3]Chemical and Environmental Engineering, University of California, Riverside, Riverside, CA, United States
Emails: david@engr.ucr.edu, webpage: http://www.cee.ucr.edu/

Keywords: damage-tolerant, biocomposite, dactyl club, telson, Bouligand

ABSTRACT

High performance structural materials require a combination of adequate strength and toughness. Moreover, ongoing demands for economical and environmentally friendly solutions require new classes of materials that are durable, lightweight, and efficiently produced. Biologically mineralized composites offer inspiration for the design of next generation structural materials due to their low density, high strength and high toughness currently unmatched by engineering technologies. Such properties are based on the ability for the organism to self-assemble fibrous organic matrices, which then act as templates for the controlled mineralization process, yielding hierarchical architectures with well-defined compositional gradients. The stomatopod (crustacean) dactyl appendage and telson are two examples of exceptionally damage-tolerant bio-composite materials that can deliver and withstand, respectively, repeated impacts up to 1500 N from one of the fastest striking events observed in nature. These materials resist catastrophic failure while enduring substantial stresses from direct impact and subsequent cavitation. Here, we report on structure-mechanical property relationships of these tough biomineralized composite materials. Using a combination of high resolution microscopy, nanomechanical testing, and modeling/simulation, we identify helicoidal and sinusoidally-modified helicoidal fibrous micro-architectures that provide enhanced toughness through stress redistribution and crack twisting. A nanoparticulate surface layer is also identified, which is found to provide stress delocalization under compressive loading. These results provide new insights to the design of impact resistant and damage-tolerant composite materials, which are also demonstrated in biomimetic composites fabricated by 3D printing and traditional layup processing.

1 INTRODUCTION

Nature's ability to fabricate hierarchical structures while controlling the multi-scale organization of organic and inorganic components has resulted in a diversity of materials that exhibit a wide range of mechanical properties and fulfill numerous functions [1,2]. One such structure is the hammer-like raptorial appendage (dactyl club) of the stomatopod (marine crustacean), *Odontodactylus scyllarus* (Figure 1A). This species employs its dactyl clubs (Figure 1B) to aggressively hunt and strike its prey, which include mollusks, crabs, and other highly mineralized organisms, with tremendous force and speed [3]. The dactyl club can break through the mechanically tough exteriors of its prey while enduring thousands of repetitive high-energy strikes and cavitation at the impact surface without catastrophically failing [3].

The stomatopod dactyl club is a multi-regional composite material that contains an organic matrix composed of chitinous fibers and an inorganic phase composed of amorphous and crystalline mineral [4]. The interior of the club, which can be divided into the periodic and striated regions, features chitinous fibers arranged in helicoidal (Bouligand) and sheet-like arrangements respectively. These regions contain amorphous calcium carbonate and calcium phosphate. In addition, the club features a stiff and hard outer region that contains a highly oriented crystalline apatitic mineral phase. Much of the success of this material in resisting catastrophic failure has been attributed to the periodic region, which has been identified as the primary-energy absorbing layer. However, details concerning the micro and nano-architecture of the hard and stiff crystalline outer impact region have not yet received full attention. This region is the first site of impact and must be able to withstand incredibly high compressive stresses from impact as well as cavitation without failing, thus warranting further examination. Here, we interrogate the micro and nano-structural features and mechanical properties of the impact region to ascertain the functional role of this region and its contribution to the overarching success of this impact-resistant and damage-tolerant natural composite material.

In conjunction with the dactyl club, O. scyllarus also relies on a shield-like segment of exoskeletal armor called the telson, which is used as a barrier to defend its burrow from predators as well as a shield during ritualized fighting with other stomatopods [5,6]. The telson can endure repeated direct blows from the dactyl clubs of conspecifics without catastrophically failing, which is suggestive of a similarly impressive and robust design. Details however regarding the ultrastructural features, chemical composition, mechanical properties, and mechanisms underlying the telson's resistance to high-energy impact loading have not yet been uncovered. In this work, we seek to uncover structure-mechanical property relationships of the stomatopod telson and draw comparisons to those of the dactyl.

2 RESULTS & DISCUSSION

2.1 Characterization of the dactyl impact region

Multi-length-scale structural features of the dactyl impact region were initially examined. Backscattered electron microscopy of a polished transverse cross-section of the dactyl club (Figure 1C) reveals its multi-regional nature, including the highly mineralized outer layer, which we term the impact region. Optical microscopy of the polished cross-section (Figure 1D) also corroborates the multi-regional nature of stomatopod dactyl club, revealing the impact and periodic regions. Additionally, the differential interference contrast imaging mode shows that the impact region can be divided into two distinct subdomains: the bulk, which comprises the majority in thickness of the impact region (typically 300 to 500 μm) and a thin surface layer, which is approximately 60 to 80 μm in thickness. We term this outermost layer the impact surface in conjunction with observations previously made by Weaver et al [4]. Figure 1D also highlights the abrupt interfaces separating the bulk of the impact region and the impact surface as well as the impact and periodic regions. A well-defined and highly ordered herringbone pattern is observed within the bulk impact region, which indicates varying orientation of the apatite crystallites as well as, potentially, a well-ordered underlying microstructure. Synchrotron x-ray diffraction studies of the impact region previously showed that the apatite crystallites have a preferred orientation with the (002) planes aligned parallel to the club surface [4]. However, the contrast observed in Figure 1D is suggestive of a more sophisticated texturing scheme of the apatitic mineral phase than was previously described. Although these striations are most evident within the bulk of the impact region, the herringbone pattern also appears to continue into the impact surface region, possibly an indication of a structural gradient across the bulk-impact surface interface. We also note that the apparent wavelength of the herringbone/sinusoid is fairly constant (45-50 μm); however, the amplitude is graded and increases from 70 μm at the periodic/impact region interface to 100 μm at the impact surface.

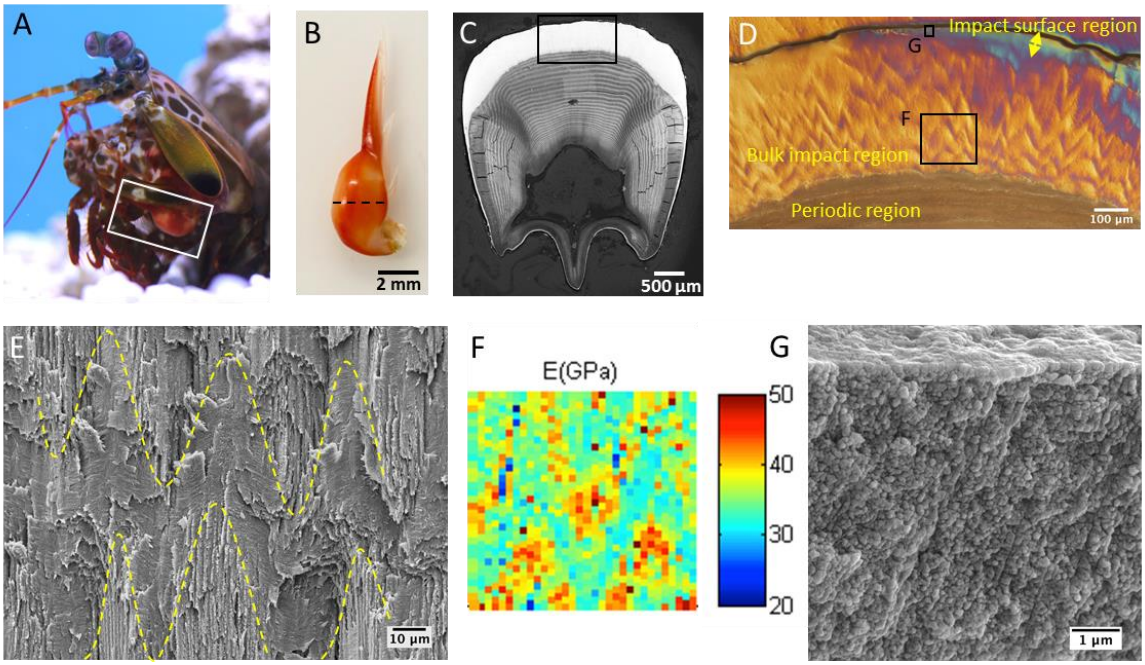

Figure 1. Stomatopod dactyl club overview and characterization of the impact region. (A) Anterior of *O. scyllarus* with dactyl segment highlighted by white box. (B) Dactyl club separated from the raptorial appendage. Dashed line indicates transverse plane of cross-section. (C) Backscattered electron micrograph of a polished transverse cross-section of the dactyl club. (D) Differential interference contrast optical micrograph of region marked in (C) highlighting the impact surface, bulk impact, and periodic regions. (E) Scanning electron micrograph (SEM) showing the fractured cross-section of the bulk impact region. Dashed lines indicate interfaces between fibers transitioning from in-plane to out-of-plane orientation. (F) High resolution nanoindentation map from region denoted in (D) showing local reduced elastic modulus as a function of position. Note the correlation between the mechanical properties and the observed herringbone pattern in the optical micrograph. (G) SEM of the impact surface, as shown in (D), revealing the nanoparticulate morphology.

The dactyl club was subsequently mechanically fractured along the sagittal plane and examined by scanning electron microscopy (SEM) to interrogate the microstructural features. Closer inspection at the impact-periodic region interface (data not shown here) shows the contrasting microstructures between the periodic and impact regions. The fractured surface of the periodic region shows a laminated microstructure characteristic of a Bouligand arrangement of mineralized chitin fibers. This helicoidal arrangement of fibers is a common design found in most arthropod cuticles [7,8]. Subsequent examination of the bulk of the impact region (Figure 1E) reveals the herringbone pattern, which correlates with optical observations made in Figure 1D. Higher magnification imaging of the bulk of the impact region reveals what appears to be a modified Bouligand structure. Fibers continue to rotate in the plane of the page; however, individual periods of rotation appear to be compacted in the azimuthal direction to form the herringbone pattern. Dashed lines indicate the transitional zones from mineralized fibers oriented in the plane of fracture and out of the plane of fracture. Examination of in-plane oriented fibers at high magnification reveals that the fibers average 49 ± 13 nm in diameter.

In addition, interspersed between the helicoidally arranged fibers are vertically aligned pore canal tubules, which are also composed of alpha-chitin fibers and remain in a fixed orientation normal to the surface of the dactyl club. These tubules not only function as transport channels for delivery of nutrient and mineral ions during molting/mineralization, but are also responsible for the observed anisotropic mechanical properties (i.e. higher elastic modulus and hardness in the direction of loading)

[9]. Similar tubular structures such as those found in bone, teeth and horns have been found to enhance toughness through mechanisms such as crack deflection and resistance to microbuckling [10]. Transmission electron microscopy (TEM) and electron diffraction analysis of the impact region (data not shown here) reveal that the apatite crystallites are highly textured with c-axis orientation preferentially aligned parallel to the alpha-chitin fiber long-axis [11]. Highly textured c-axis aligned mineral found within the pore canal fibers, which are oriented normal to the club surface, are likely responsible for the observed higher elastic modulus and hardness in the loading direction.

High resolution nanoindentation mapping was used to ascertain the local elastic modulus and hardness within the impact region and impact surface. The highest reported values for modulus and hardness occur within the impact surface region nearest to the club surface and reach approximately 60 GPa and 3 GPa, respectively. Figure 1F depicts a high resolution nanoindentation map of the bulk impact region. Indents were loaded in displacement control. The indentation map shows a strong correlation with the observed herringbone pattern from DIC imaging and SEM analyses. The reduced modulus oscillates between approximately 30 GPa and 45 GPa corresponding with the local fiber orientation within the microstructure. We hypothesize that areas of higher modulus correlate to the interrogation of fibers that are oriented out of the plane of section. Similarly, lower values of reduced modulus likely result from probing fibers that are oriented parallel to the plane of section. This is due not only to the mechanical anisotropy of the chitinous fibers, but also due to the high degree of crystallographic texturing [4,11].

Analysis of the impact surface region from the same fractured sample is shown in Figure 1G. Remnants of a herringbone-like architecture are apparent within the impact surface layer (not shown); however, moving across the interface from the bulk into the impact surface region, we observe a gradual transition in morphology from helicoidally arranged fibers to densely packed nanoparticles. These nanoparticles have an average diameter of 64 ± 12 nm. Subsequent TEM and electron diffraction characterization (data not shown) reveal that these nanoparticles are single crystalline, randomly oriented grains of hydroxyapatite [11].

To understand the roles of the herringbone architecture and the nano-particulate impact surface on the damage tolerance of the dactyl, a combination of finite element (FE) analysis, simulation, 3D printing and mechanical testing were used. Models were first developed to represent the traditional Bouligand and herringbone-modified Bouligand structures. FE analysis was used to compare the responses of the two architectures to uniaxial compressive strain, which was applied in the z-direction (same direction of loading as in the natural system). Analysis of the surfaces of constant normalized von Mises stress (data not shown) show that the herringbone structure allows for a greater redistribution of stresses compared to the helicoidal design. These results were further corroborated by uniaxial compression testing on 3D printed mimics of the herringbone and Bouligand designs. The parts were fabricated using a multi-material 3D printer, where a rigid polymer was used to mimic the fibers and a softer, elastomeric polymer was used to mimic the matrix. Examination of the stress-strain curves (data not shown) for the compression tests, show that the strain-to-failure for the herringbone structure is approximately twice as high as that of the Bouligand structure. This confirms that the herringbone architecture allows for better energy absorption capabilities than the Bouligand motif, and can be attributed to the flattening of sinusoidal fiber layers upon compressive loading.

High load nanoindentation in combination with FE simulation was also used to understand the role of the nanoparticulated impact surface on the mechanical response of the dactyl club. Quasi-static indentations to varying peak loads were placed within regions of a polished coronal (parallel to the club surface) section containing the impact surface layer and with the impact surface layer removed (only contacting the bulk impact region). SEM characterization of the indents placed within the nanoparticulate impact surface layer shows substantial pile up of material surrounding the faces of the indents, which resembles the shear-banding phenomenon observed in metals and other ductile materials. A representative micrograph of a 5 μm displacement indent is shown in Figure 2B. In contrast, indents within the bulk impact region (i.e., with the impact surface removed) are smooth-

faced and plastic-looking with no observable pile-up (e.g., Figure 2C). This leads us to hypothesize that the pile up behavior is a result of meso-scale displacement of the isotropic particles within the impact surface. This motion may have implications for the redistribution of stress during impact loading. The ability for plastic deformation of the impact surface layer through particle motion may be critical for preventing stress concentration during impact loading. To confirm this hypothesis, FE simulations were conducted. A model consisting of an isotropic particulate layer placed over an isotropic homogeneous substrate with similar material properties was loaded in compression. The von Mises stress distribution was examined for cases where the Young's modulus ratios between the particle and matrix were varied from 1:1, 1:10, 1:100, and 1:1000. The results showed that for increasing ratio of Young's modulus, the stress is confined within the particulate impact surface layer, which supports our preliminary hypothesis concerning the role of particles in redistributing stress.

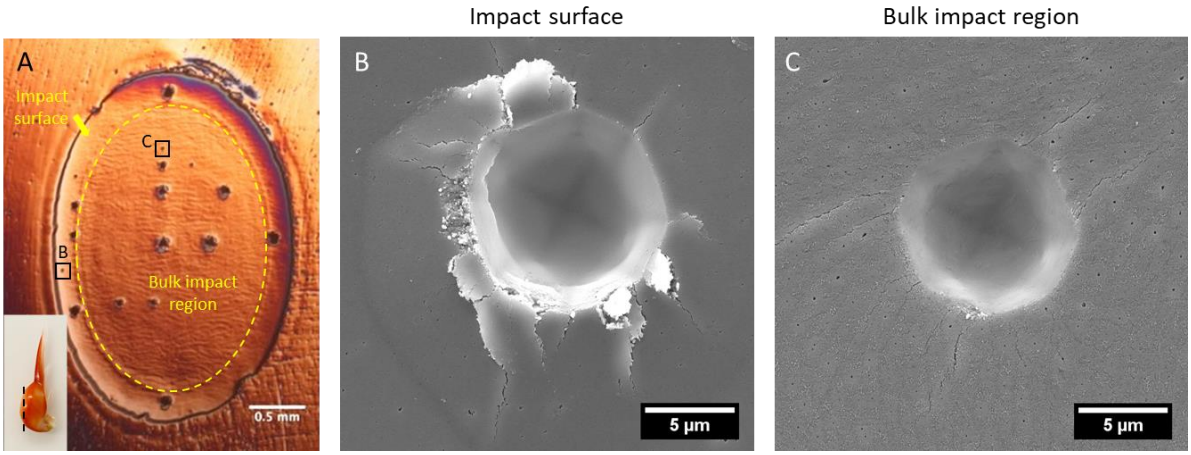

Figure 2. High load nanoindentation within the impact surface and bulk impact region. (A) DIC optical micrograph of a polished coronal cross-section of the dactyl club revealing the impact surface and bulk impact region. Inset showing plane of cross-section within the dactyl. (B) SEM micrograph of a 5 µm displacement indent placed within the impact surface. (C) SEM micrograph of a 5 µm displacement indent placed within the bulk impact region. Indented areas in (B) and (C) are denoted in (A).

2.2 Characterization of the stomatopod telson

Optical microscopy of bulk specimens as well as polished cross-sections of the stomatopod telson was initially conducted to identify macrostructural features of the telson. Figure 3 presents an overview of these macro-morphological features. Figure 3A shows an overview of the dissected telson structure. The telson for *O. scyllarus* varies in size with the age of the animal; however, it is shown here to be approximately 20 mm in width and 22 mm in length. Noticeable macro-morphological features include well-developed spines and apparent teeth that terminate each spine. Cross-sectional analysis of the telson (Figure 3B) shows a highly contoured concave morphology with several ridges lining the dorsal cuticle (denoted by black arrows). These ridges are more commonly referred to as carinae, the largest of which is the medial carina and lies along the centerline of the telson. A higher magnification dark field micrograph of the telson cuticle along the medial plane and carina (boxed area in Figure 3B) is shown in Figure 3C. We note the laminated appearance and nested bands within the cuticle, which resembles the periodic region of the dactyl club and is indicative of a Bouligand micro-architecture. It is also worth noting that there is a densely packed laminated area near the outer surface of the cuticle, which comprises the exocuticle and is approximately 100 µm thick. The underlying set of laminations, beneath the exocuticle, comprises the endocuticle and is much thicker (approximately 500 µm).

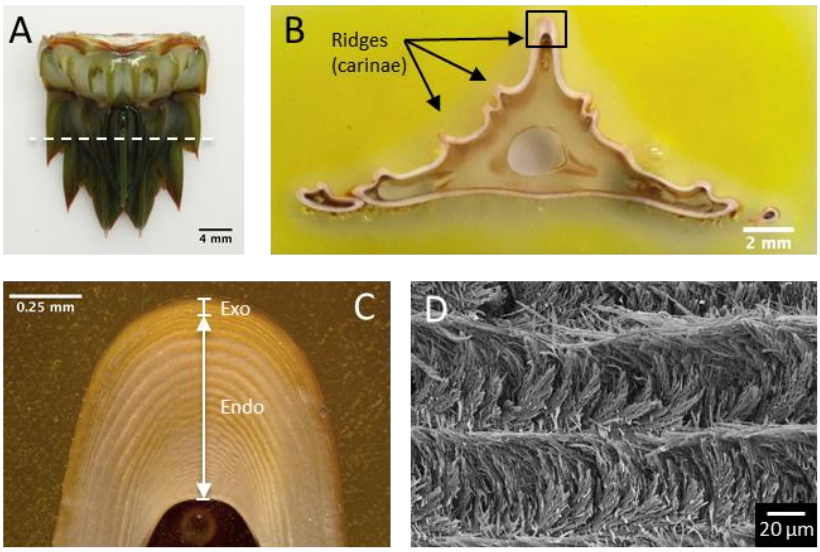

Figure 3. Macro-morphology and microstructure of the stomatopod telson. (A) Overview image of the telson segment of *O. scyllarus*. (B) Optical image of a polished transverse cross-section, along the plane denoted in (A), of the telson. (C) Higher magnification optical micrograph of the medial carina (area denoted by box in (B)). (D) SEM micrograph of the endocuticle revealing the Bouligand architecture of alpha-chitin fibers.

Microstructural features of the telson structures were subsequently examined by SEM analysis of fractured and polished cross-sectional specimens. Figure 3D shows a fractured surface SEM micrograph of a region of the endocuticle along the medial carina. Close inspection reveals that the telson structure features the common Bouligand arrangement of fibers characteristic of the arthropod cuticle. The exocuticle also consists of a densely packed arrangement of mineralized fibers whereby these fibers rotate about an axis that is normal to the telson surface and parallel to the plane of the image. We note that the fiber bundles within the endocuticle are less densely packed than in the exocuticle, which is also a common feature of the arthropod cuticle.

Additional characterization of the microstructure along lateral carinae as well as flat non-ridged regions reveal microstructural differences, namely the number of periods of rotation, the rotation pitch length as a function of distance from the surface (pitch gradient) and the overall cuticle thickness. Future work will seek to understand the role of these microstructural differences, as well as the role of macrostructural features, namely cross-sectional geometry, on the mechanical response of the telson when subjected to impact.

3 CONCLUSION

The results described herein confirm that the stomatopod dactyl club is a highly sophisticated multi-regional composite material that has been optimized to resist failure from high energy impacting events. Within the impact region of the dactyl club, we have identified a unique herringbone-modified Bouligand architecture, featuring sinusoidally arranged helicoidal alpha-chitin fibers mineralized with highly crystalline and textured hydroxyapatite. This architecture was found to provide enhanced stress redistribution and energy absorption in response to compressive loading as compared to the traditional Bouligand design. We also identified a thin surface layer composed of isotropic randomly oriented nanoparticulate grains of hydroxyapatite. High load nanoindentation and FE simulation suggest that this layer may provide an additional advantage of stress confinement and delocalization upon impact loading. The stomatopod telson, which is also capable of withstanding high energy impacts from the

dactyl, features a similarly robust helicoidal fibrous micro-architecture. Combined with a corrugated-like macro-morphology, these features may be responsible for providing adequate bulk stiffness yet, at the same time, energy absorption for resisting catastrophic failures from high velocity impacts.

ACKNOWLEDGEMENTS

The authors would like to acknowledge financial support from the Air Force Office of Scientific Research (AFOSR-FA9550-12-1-0245) and the Air Force Office of Scientific Research, Multi-University Research Initiative (AFOSR-FA9550-15-1-0009). This research was conducted with Government support under and awarded by DoD, Air Force Office of Scientific Research, National Defense Science and Engineering Graduate (NDSEG) Fellowship, 32 CFR 168a.

REFERENCES

[1] M. A. Meyers, P.-Y. Chen, A. Y.-M. Lin, Y. Seki, Biological materials: Structure and mechanical properties. *Progress in Materials Science* **53**, 1-206 (2008).
[2] P.-Y. Chen, J. McKittrick, M. A. Meyers, Biological materials: Functional adaptations and bioinspired designs. *Progress in Materials Science* **57**, 1492-1704 (2012).
[3] S. N. Patek, R. L. Caldwell, Extreme impact and cavitation forces of a biological hammer: strike forces of the peacock mantis shrimp Odontodactylus scyllarus. *Journal of Experimental Biology* **208**, 3655-3664 (2005).
[4] J. C. Weaver *et al.*, The stomatopod dactyl club: a formidable damage-tolerant biological hammer. *Science* **336**, 1275-1280 (2012).
[5] J. R. Taylor, S. N. Patek, Ritualized fighting and biological armor: the impact mechanics of the mantis shrimp's telson. *J Exp Biol* **213**, 3496-3504 (2010).
[6] R. Caldwell, H. Dingle, Ecology and evolution of agonistic behavior in stomatopods. *Naturwissenschaften* **62**, 214-222 (1975).
[7] P. Romano, H. Fabritius, D. Raabe, The exoskeleton of the lobster Homarus americanus as an example of a smart anisotropic biological material. *Acta Biomaterialia* **3**, 301-309 (2007).
[8] E. A. Zimmermann *et al.*, Mechanical adaptability of the Bouligand-type structure in natural dermal armour. *Nature Communications* **4**, 2634 (2013).
[9] S. Amini *et al.*, Textured fluorapatite bonded to calcium sulphate strengthen stomatopod raptorial appendages. *Nat Commun* **5**, 3187 (2014).
[10] J. McKittrick *et al.*, Energy absorbent natural materials and bioinspired design strategies: A review. *Materials Science and Engineering: C* **30**, 331-342 (2010).
[11] N. A. Yaraghi *et al.*, A Sinusoidally Architected Helicoidal Biocomposite. *Adv Mater* **28**, 6835-6844 (2016).